Appl. Numer. Math. 203 (2024) 255–268

Contents lists available at ScienceDirect

Applied Numerical Mathematics

journal homepage: www.elsevier.com/locate/apnum

Research Paper

Analysis of a line method for reaction-diffusion models of nonlocal type

Domenico Mezzanotte [a,*,1], Donatella Occorsio [b,c,1], Ezio Venturino [a,1]

[a] Department of Mathematics "Giuseppe Peano", University of Turin, Via Carlo Alberto 10, 10123, Turin, Italy
[b] Department of Mathematics, Computer Science and Economics, University of Basilicata, Viale dell'Ateneo Lucano 10, 85100, Potenza, Italy
[c] Istituto per le Applicazioni del Calcolo "Mauro Picone", Naples branch, C.N.R. National Research Council of Italy, Via P. Castellino 111, 80131, Naples, Italy

ARTICLE INFO

Keywords:
Reaction diffusion equations
Line method
Generalized Bernstein polynomials

ABSTRACT

The considerable interest in the recent literature for nonlocal equations and their applications to a wide range of scientific problems does not appear to be supported by a corresponding advancement in the efforts toward reliable numerical techniques for their solution. The aim of this paper is to provide such an algorithm and above all to prove its high order convergence. The numerical scheme is applied to a diffusion problem in a biological context, arising in population theory. Several simulations are carried out. At first the empirical order of convergence on examples with known solution is assessed. Their results are in agreement with the theoretical findings. Simulations are then extended to cases for which the solution is not known a priori. Also in this case the outcomes support the convergence analysis.

1. Introduction

In relatively recent years there has been a considerable interest in the study of situations incorporating nonlocal effects arising in engineering, specifically for instance in heterogeneous material science [9], diffusion [19], modified phase fields [5,10], Allen-Cahn [11] and Cahn-Hillier [20] equations also under different boundary conditions, [7,8]. Traveling waves in this context have been considered in [15] as well as the possibility of nonuniqueness of the solutions, [16]. The idea has then been extended also to models in population biology. Since a century, populations interaction has been the thrust behind the development of population theory, initially through models depending only on time and subsequently also on space, see for instance [29,1]. In this context, historically the classical studies of Fisher [23] and [27] on population waves propagation play a major role, as well as more recent investigations, see e.g. [26,40].

In more recent years a revived attention on variations of the reaction-diffusion equations including integro-differential terms, [6,42] and delays [38] has arisen. It is to be remarked that these studies could lead to spatiotemporal heterogeneities [17,29,25]. Determination of the speed of invasions is also relevant from a biological point of view, [32], in particular for the control of pests and invasive alien species [12]. These investigations are important because they pave the way to relevant applications in mathematical biology [37] and medicine [13].

* Corresponding author.
E-mail addresses: domenico.mezzanotte@unito.it (D. Mezzanotte), donatella.occorsio@unibas.it (D. Occorsio), ezio.venturino@unito.it (E. Venturino).
[1] Member of the Gruppo Nazionale Calcolo Scientifico-Istituto Nazionale di Alta Matematica (GNCS-INdAM) and of the Research ITalian network on Approximation (RITA).

https://doi.org/10.1016/j.apnum.2024.05.011
Received 1 December 2023; Received in revised form 6 March 2024; Accepted 10 May 2024

Available online 15 May 2024

Numerical methods such as the finite difference method and the finite element method for standard reaction-diffusion models without nonlocalities are well known in the literature. Conversely, even though models including nonlocalities are frequently used [4], to our knowledge there is little information on the numerical schemes used to generate the simulations. In this paper we would like to address this issue, particularly focusing on specific reaction-diffusion equations. In the previous work [31], we proposed a line method for the integration of a simple nonlinear reaction-diffusion equation. The numerical experiments reveal that an empirical fourth-order convergence order is attained. The purpose of this investigation is the analytic assessment of this result for a relevant model of biological nature. In particular, a few instances of the latter will also be considered for the numerical experiments in support of the theoretical findings.

The paper is organized as follows. Section 2 collects some preliminaries useful for the numerical treatment of the model described in Section 3. We introduce the numerical scheme to discretize the equation under study in Section 4, while Section 5 is devoted to its error analysis. Finally, in Section 6 we present and comment on several numerical simulations to prove the effectiveness of the proposed method.

2. Preliminaries

In what follows the notation $g_x(y)$ has to be understood in the sense that any bivariate function $g(x,y)$ is considered to depend only on the variable y. Moreover, C denotes a positive constant, which may have different values at different occurrences, and we write $C \neq C(n,f,\ldots)$ to mean that $C>0$ is independent of $n, f, \ldots$. Finally, for sake of brevity we introduce the notation

$$\boldsymbol{x} = (x_0, x_1, \ldots, x_{n-1}, x_n) \in \mathbb{R}^{n+1}.$$

In what follows $C^0([-a,a])$ denotes the space of the continuous functions, equipped with the uniform norm $\|f\| := \max_{x\in[-a,a]} |f(x)|$.

In $C^0([-a,a])$, let us consider the following Sobolev-type subspaces defined for any integer $s \geq 1$ as

$$W_s([-a,a]) = \left\{ f \in C^0([-a,a]), f^{(s-1)} \in \mathcal{AC} : \|f^{(s)}\phi^s\| < \infty \right\}, \quad \phi(x) = \sqrt{a^2 - x^2},$$

where $\mathcal{AC}$ denotes the space of all absolutely continuous functions on every closed subset of $(-a,a)$. The space $W_s([-a,a])$ is equipped with the norm

$$\|f\|_{W_s} = \|f\| + \|f^{(s)}\phi^s\|.$$

In any $f \in C([-a,a])$ the n-th Bernstein polynomial $B_n f$ is defined as [22,36]

$$B_n f(x) := \sum_{j=0}^{n} p_{n,j}(x) f(x_j), \quad x_j := -a + jh, \quad h = \frac{2a}{n}, \quad x \in [-a,a], \tag{1}$$

where

$$p_{n,j}(x) := \binom{n}{j} \left(\frac{a+x}{2a}\right)^j \left(\frac{a-x}{2a}\right)^{n-j}. \tag{2}$$

Let us fix $\ell \in \mathbb{N}$, we recall the definition of the n-th Generalized Bernstein (GB) polynomial of parameter ℓ, namely the polynomial $B_{n,\ell} f$, that takes the following expression

$$B_{n,\ell} f(x) = \sum_{j=0}^{n} p_{n,j}^{(\ell)}(x) f(x_j), \quad \text{with} \quad p_{n,j}^{(\ell)}(x) = \sum_{i=0}^{m} p_{n,i}(x) c_{i,j}^{(n,\ell)}, \tag{3}$$

where $c_{i,j}^{(n,\ell)}$ are the entries of the matrix $C_{n,\ell} \in \mathbb{R}^{(n+1)\times(n+1)}$

$$C_{n,\ell} = \mathbf{I} + (\mathbf{I} - \mathbf{A}) + \ldots + (\mathbf{I} - \mathbf{A})^{\ell-1}, \quad C_{n,1} = \mathbf{I}, \tag{4}$$

$\mathbf{I}$ being the identity matrix of order $n+1$ and $\mathbf{A}$ being defined as

$$\mathbf{A} := (\mathbf{A}_{i,j}), \qquad \mathbf{A}_{i,j} := p_{n,j}(x_i), \quad i,j \in \{0,1,\ldots,n\},$$

with $p_{n,j}(x)$ defined as in (2).

Other representations of the GB polynomial are available in the literature, such as the one based on their eigenstructure (see e.g. [14,18]). Nevertheless, the choice of expression (3) for the GB polynomial is optimal since it allows to consider $B_{n,\ell}$ as the n-th classical Bernstein polynomial B_n of a function g having a suitable sampling vector, i.e. $B_{n,\ell} f(x) = B_n g(x) = \boldsymbol{p}_n(x)\boldsymbol{g}_n$, where $\boldsymbol{g}_n := C_{n,\ell}\boldsymbol{f}_n$ with $\boldsymbol{p}_n(x) = [p_0(x), \ldots, p_n(x)]^T$ and $\boldsymbol{f}_n = [f(x_0), \ldots, f(x_n)]^T$. Consequently, the GB polynomial $B_{n,\ell} f$ can be computed by using the well-known de Casteljau recursive scheme that is fast and stable [21, §3]. A complete survey on the Generalized Bernstein polynomials and their applications can be found in [34,36].

We recall the following *GB* rule based on the Generalized Bernstein polynomials $B_{n,\ell}f$ [22,31,35]

$$\int_{-a}^{a} f(y)\varphi(y-x)\,dy = \int_{-a}^{a} B_{n,\ell}(f\varphi_x,y)\,dy + \int_{-a}^{a}[f(y)\varphi_x(y) - B_{n,\ell}(f\varphi_x,y)]\,dy$$
$$= \sum_{j=0}^{n} f(x_j)\varphi(x_j-x)D_j^{(\ell)} + e_{n,\ell}(f\varphi_x) =: \mathcal{K}_{n,\ell}(f,x) + e_{n,\ell}(f\varphi_x), \tag{5}$$

where

$$D_j^{(\ell)} = \frac{2a}{n+1}\sum_{i=0}^{n} c_{i,j}^{(n,\ell)}, \quad x_j := -a + jh, \quad h = \frac{2a}{n}. \tag{6}$$

As far as the error of the *GB* rule is concerned, we recall the following result [31,35]

Theorem 2.1. *Under the assumption*

$$\sup_{x\in[-a,a]} (f\varphi_x) \in W_s([-a,a]), \quad 1 \le s \le 2\ell,$$

we have

$$\sup_{x\in[-a,a]} |e_{n,\ell}(f\varphi_x)| \le C\left(\frac{a^{s+1}\mathcal{M}}{(\sqrt{n})^s}\right), \quad C \ne C(n,f,\varphi), \tag{7}$$

where

$$\mathcal{M} := \sup_{x\in[-a,a]} \|f\varphi_x\|_{W_s}.$$

Remark 2.2. By (7), under the assumptions of Theorem 2.1, we have

$$\sup_{x\in[-a,a]} |e_{n,\ell}(f\varphi_x)| \sim \mathcal{O}(h^{s/2}).$$

3. The model

Models for the study of population growth, interactions and evolutions are very well known. As explained in the Introduction, the first ever population P model proposed was by Malthus [30] at the end of the eighteenth century, as a very simple ordinary differential equation, in which r denotes the per capita growth rate:

$$\frac{dP(t)}{dt} = rP(t),$$

with later improvements by Verhulst [39] that correct the false consequences of the former, preventing that in a finite environment a population P can continue to grow exponentially without bounds:

$$\frac{dP(t)}{dt} = rP(t)\left(1 - \frac{P(t)}{K}\right).$$

Here K denotes the carrying capacity of the environment, how many individuals P the environment can sustain; its reciprocal K^{-1} can also be seen as a measure of intraspecific competition. The solutions of the model indeed tend to this finite value K. Lotka and Volterra [28,41] proposed the first models for populations interactions about a century ago. Diffusion in space was introduced in later researches, with the classical results of Fisher on the development of population waves [23] in space time, [29]. In this situation, the population u is a function of both space and time, $u = u(x,t)$.

Population theory in biology is nowadays a well established branch of scientific research. The omnicomprehensive book of Murray [33] presents a wide spectrum of problems and applications. In this light, we consider here a one population model in which diffusion is combined with a more recent observation, that something happening in a certain location in space can affect populations residing even at long distances from the occurrence of the perturbation. These nonlocal models have been investigated in the literature in other fields, but to our knowledge the application to mathematical population theory is novel, with the exception of our earlier investigation [31].

Consider the following integrodifferential equation for the time evolution of a population on a spatial domain:

$$\frac{\partial u(x,t)}{\partial t} = \frac{\partial^2 u(x,t)}{\partial x^2} + r\mathcal{K}(u,x,t) - m(x)u(x,t), \tag{8}$$

where $\mathcal{K}(u,x,t)$ represents a non-local operator defined by

$$\mathcal{K}(u,x,t)=\int_{-a}^{a}\varphi(y-x)u(y,t)\,dy, \tag{9}$$

with $\varphi(y-x)$ sufficiently smooth. A few assumptions are in order. The population reproduction rate $r\geq 0$ is constant, and the mortality $m(x)\in C([-a,a])$, $m(x)\geq 0\,\forall x\in[-a,a]$ depends on the spatial location.

In what follows we will devise a numerical scheme for solving the equation in (8) subject to the initial conditions

$$u(x,0)=k(x)\geq 0,\quad k\in C([-a,a]), \tag{10}$$

and to the Dirichlet boundary conditions

$$u(-a,t)=b_{-}(t)\geq 0,\quad u(a,t)=b_{+}(t)\geq 0,\quad t>0,\quad b_{\pm}\in C([0,\infty)), \tag{11}$$

where $k(x)$ and $b_{\pm}(t)$ are known functions.

To be specific from the ecological point of view, the model assumes that available food is always abundant, justifying the use of a kind of Malthus law in the formulation, and the reproduction is influenced at a distance. In the latter situation for instance, feeding in good pastures for wandering herbivores may lead to the appearance of newborns in other areas.

4. The numerical method

To determine an approximate solution of equation (8), we propose here a "method of lines". To describe the numerical procedure, we start by considering the following spatial mesh of $n+1$ equally spaced nodes

$$\mathcal{X}=:\left\{x_i=-a+hi,\quad i=0,1,\dots,n,\quad h=\frac{2a}{n}.\right\}$$

By collocating equation (8) at the $n-1$ internal nodes $\{x_i\}_{i=1}^{n-1}$, and employing the boundary conditions (11) to assess the solution values at the endpoints $x_0=-a$ and $x_n=a$, the restrictions of the solution at the internal nodes x_i become univariate functions depending only on time t. Hence, setting

$$\begin{aligned}
&u_i(t):=u(x_i,t),\quad \left.\frac{\partial u(x,t)}{\partial t}\right|_{x=x_i}=:u_i'(t)\\
&\frac{\partial^2 u(x,t)}{\partial x^2}=:D_{xx}u(x,t),\quad \left.\frac{\partial^2 u(x,t)}{\partial x^2}\right|_{x=x_i}=:D_{x_ix_i}u(t),\\
&\boldsymbol{u}(t)=[u_1(t),\dots,u_{n-1}(t)]^T,\quad \boldsymbol{D}_{xx}\boldsymbol{u}(t)=[D_{x_1x_1}u(t),D_{x_2x_2}u(t),\dots,D_{x_{n-1}x_{n-1}}u(t)]^T,\\
&\mathcal{K}(\boldsymbol{u},t)=[\mathcal{K}(u,x_1,t),\dots,\mathcal{K}(u,x_{n-1},t)]^T,\quad \mathcal{K}(u,x_i,t)=\int_{-a}^{a}\varphi(y-x_i)u(y,t)dy,\\
&\mathcal{M}(\boldsymbol{u},t)=[m(x_1)u_1(t),\dots,m(x_{n-1})u_{n-1}(t)]^T,
\end{aligned} \tag{12}$$

we obtain the following system of ordinary differential equations depending only on the time t, written in compact form:

$$\boldsymbol{u}'(t)=\boldsymbol{D}_{xx}\boldsymbol{u}(t)+r\mathcal{K}(\boldsymbol{u},t)-\mathcal{M}(\boldsymbol{u},t). \tag{13}$$

Now, the numerical approach we propose here consists in the following steps:

1. to discretize the second partial derivatives in space by finite difference schemes;
2. to approximate the integrals $\mathcal{K}(\boldsymbol{u})$ by the GB rule recalled in Section 2, thus obtaining an "approximate" ordinary differential equations (ODEs) system of the first order;
3. to apply to this "approximate" ODEs system thus obtained the Runge-Kutta-Fehlberg scheme of order (4,5).

To preserve the accuracy $\mathcal{O}(h^4)$ of the Runge-Kutta scheme, steps 1-2 have to be performed in a clever way that we now describe.

Step 1 The finite difference schemes approximating the second partial derivatives are of order $\mathcal{O}(h^4)$ (see e.g. [24]). We use different formulae, according to the points that are internal or "close" to the boundary. To be more precise, we make use of the five points classical central finite difference scheme (see e.g. [24]) at the nodes x_i, $i=2,\dots,n-2$. At the points x_1 and x_{n-1} finite difference formulae are employed that are subject to two constraints. They must use only nodes in the mesh and must retain the same fourth-order accuracy as the classical ones. Such formulae can be constructed by the method of the undetermined coefficients [2,3], or simply found in tables.

Step 2 The integrals $\mathcal{K}(u,x_i,t)$ are discretized by the GB quadrature formula (5) described in Section 2, i.e.

$$\mathcal{K}_{n,\ell}(u,x_i,t)=\sum_{j=0}^{n}\varphi(x_j-x_i)u(x_j,t)D_j^{(\ell)}, \tag{14}$$

Assuming that the integrand belongs to be the Sobolev space $W_s([-a,a])$, the order accuracy of the rule is $\mathcal{O}(h^{s/2})$. Hence for smooth φ_x the rate of convergence is generally larger than $\mathcal{O}(h^4)$.

About the discretized additional conditions, note that from (10) they become

$$u_i(0) = k(x_i), \quad i = 0, \dots, n. \tag{15}$$

At the endpoints $\pm a$ the boundary conditions (11) are employed providing the remaining two equations

$$u_0(t) = b_-(t), \quad u_n(t) = b_+(t). \tag{16}$$

Now, setting

$$\begin{aligned}
\widetilde{D}_{x_1x_1}u(t) &:= \frac{1}{h^2}\left[\frac{5}{6}u_0(t) - \frac{5}{4}u_1(t) - \frac{1}{3}u_2(t) + \frac{7}{6}u_3(t) - \frac{1}{2}u_4(t) + \frac{1}{12}u_5(t)\right],\\
\widetilde{D}_{x_ix_i}u(t) &:= \frac{1}{h^2}\left[-\frac{1}{12}u_{i-2}(t) + \frac{4}{3}u_{i-1}(t) - \frac{5}{2}u_i(t) + \frac{4}{3}u_{i+1}(t) - \frac{1}{12}u_{i+2}(t)\right],\ i = 2, \dots, n-2,\\
\widetilde{D}_{x_{n-1}x_{n-1}}u(t) &:= \frac{1}{h^2}\left[\frac{1}{12}u_{n-5}(t) - \frac{1}{2}u_{n-4}(t) + \frac{7}{6}u_{n-3}(t) - \frac{1}{3}u_{n-2}(t) - \frac{5}{4}u_{n-1}(t) + \frac{5}{6}u_n(t)\right],
\end{aligned}$$

we consider the following discretized ODEs system

$$\frac{d\widehat{u}_i(t)}{dt} = \widetilde{D}_{x_ix_i}\widehat{u}(t) + r\,\mathcal{K}_{n,\ell}(\widehat{u}, x_i, t) - m(x_i)\widehat{u}_i(t), \quad i = 1, 2, \dots, n-1, \tag{17}$$

which can be rewritten in compact form as follows

$$\widehat{\boldsymbol{u}}\,'(t) = \widetilde{\boldsymbol{D}}_{xx}\widehat{\boldsymbol{u}}(t) + r\mathcal{K}_{n,\ell}(\widehat{\boldsymbol{u}}, t) - \mathcal{M}(\widehat{\boldsymbol{u}}, t). \tag{18}$$

5. Error analysis

The main result of this investigation concerns the convergence of the method. To this end, the theoretical analysis provides the following result:

Theorem 5.1. *The proposed discretization scheme (18) is convergent of order* 4*, namely*

$$\|\boldsymbol{u} - \widehat{\boldsymbol{u}}^*\| = \mathcal{O}(h^4).$$

Proof. Let us denote by $\widehat{\boldsymbol{u}}^*(t) := [\widehat{u}_1^*(t), \dots, \widehat{u}_{n-1}^*(t)]^T$ the solution of the system (18) computed through the Runge-Kutta-Fehlberg (4,5), we have

$$\|\widehat{\boldsymbol{u}} - \widehat{\boldsymbol{u}}^*\| = \mathcal{O}(h^4). \tag{19}$$

Now we estimate the discretization error, and by (13) and (18) we get

$$\begin{aligned}
\|\boldsymbol{u}' - \widehat{\boldsymbol{u}}'\| &\le \|\boldsymbol{D}_{xx}\boldsymbol{u} - \widetilde{\boldsymbol{D}}_{xx}\widehat{\boldsymbol{u}}\| + r\|\mathcal{K}(\boldsymbol{u}) - \mathcal{K}_{n,\ell}(\widehat{\boldsymbol{u}})\| \\
&\quad + \|\mathcal{M}(\boldsymbol{u}) - \mathcal{M}(\widehat{\boldsymbol{u}})\| =: I_1 + I_2 + I_3.
\end{aligned} \tag{20}$$

We recall that the finite differences scheme used ensures that (see [24])

$$I_1 \le Ch^4. \tag{21}$$

To estimate I_2 we use

$$I_2 \le r\left(\|\mathcal{K}(\boldsymbol{u}) - \mathcal{K}_{n,\ell}(\boldsymbol{u})\| + \|\mathcal{K}_{n,\ell}(\boldsymbol{u}) - \mathcal{K}_{n,\ell}(\widehat{\boldsymbol{u}})\|\right).$$

Assuming that $u\varphi_x$ is sufficiently smooth (say $u\varphi_x \in W_8([-a,a])$) in view of Theorem 2.1

$$\|\mathcal{K}(\boldsymbol{u}) - \mathcal{K}_{n,\ell}(\boldsymbol{u})\| \le Ch^4.$$

To estimate $\|\mathcal{K}_{n,\ell}(\boldsymbol{u}) - \mathcal{K}_{n,\ell}(\widehat{\boldsymbol{u}})\|$, consider the following inequalities

$$|\mathcal{K}_{n,\ell}(\widehat{u}, x_i, t) - \mathcal{K}_{n,\ell}(u, x_i, t)| \le \sum_{j=0}^{n} |D_j^{(\ell)}||\varphi(x_j - x_i)||u(x_j, t) - \widehat{u}(x_j, t)| \tag{22}$$

$$\le \sup_{x,t}|\varphi(x - x_i)||u(x,t) - \widehat{u}(x,t)| \sum_{j=0}^{n} |D_j^{(\ell)}| \tag{23}$$

$$\le C\|\varphi_x\|\,\|\boldsymbol{u} - \widehat{\boldsymbol{u}}\|, \quad C \ne C(n). \tag{24}$$

Table 1
Example 6.1, model (26) - Empirical order of convergence.

n	$e_n(u)$	EOC_n
8	1.91e-02	
16	3.72e-04	5.68
32	1.62e-05	4.52
64	1.70e-06	3.25
128	5.51e-07	1.63
256	1.26e-08	5.45
512	6.37e-10	4.31
$\mathrm{EOC}_{\mathrm{mean}}$		4.14

Hence, setting $\Phi = \sup_{x\in[-a,a]} \|\varphi_x\|$

$$\|\mathcal{K}_{n,\ell}(\boldsymbol{u}) - \mathcal{K}_{n,\ell}(\widehat{\boldsymbol{u}})\| \le C\Phi\|\boldsymbol{u} - \widehat{\boldsymbol{u}}\| \le C\Phi h^4. \tag{25}$$

Finally, setting $M = \sup_{x\in[-a,a]} m(x)$

$$I_3 \le CMh^4.$$

Combining the last estimate with (21), and (25) with (20), we can conclude that the discretization error behaves like $\mathcal{O}(h^4)$. □

6. Numerical examples

In this section, we perform some numerical simulations to test the effectiveness of the method on some variants of the model (8). In this context, we consider different kernel functions $\varphi(y-x)$ and various choices for the Dirichlet boundary conditions $b_{\pm}(t)$ and the initial conditions $k(x)$.

All the numerical tests are carried out in Matlab R2022a in double precision on a MacBook Pro laptop under the macOS operating system. The software developed is only a prototype, but it is available from the authors upon request.

6.1. Tests in which the solution is known a priori

First of all, we report some examples, namely Examples 6.1, 6.2 and 6.3, where the analytical solution $u(x,t)$ is known. We also fix $a = 2$ and $T = 10$ to make direct comparisons in similar contexts. Consequently, in each table, we display the maximum relative errors attained by the chosen numerical scheme for increasing values of n

$$e_n(u) = \sup_{t\in[0,T]} \max_{x\in[-a,a]} \frac{|u(x,t) - \hat{u}_n(x,t)|}{|u(x,t)|},$$

where $\hat{u}_n(x,t)$ is the numerical solution of the discretized model for a fixed number n of equally spaced points of the grid.

The tables also display the Empirical Order of Convergence (EOC_n) and the Mean Empirical Order of Convergence ($\mathrm{EOC}_{\mathrm{mean}}$), defined as follows

$$\mathrm{EOC}_n = \frac{\log\left(\frac{e_{n/2}(u)}{e_n(u)}\right)}{\log 2}, \quad \mathrm{EOC}_{\mathrm{mean}} = \frac{1}{P-2}\sum_{k=3}^{P} \mathrm{EOC}_{2^k},$$

where P denotes a fixed integer. In these cases of study we set it equal to 9.

Tables 1, 2 and 3 display the numerical results attained by the first three examples applied to the considered model. We observe that when using an equally spaced grid of 513 nodes, we manage to approximate the exact solution with around 10 exact significant digits, while the Mean Empirical Order of Convergence is always around 4. This circumstance is not surprising, since we are dealing with finite difference schemes of order 4.

In Example 6.3, note that the oscillation of the EOC_n values can be addressed to the difficulty of the example itself. On the other hand, we are comforted by the fact that the MEOC is around 4 also in this case, according to the theoretical expectations.

Example 6.1.

$$u(x,t) = x^2 t, \tag{26}$$
$$r = \frac{1}{2}, \quad \varphi(y-x) = \sin(y-x), \quad m(x) = x+3,$$
$$u(\boldsymbol{x},0) = (0,\dots,0), \quad u(-a,t) = u(a,t) = a^2 t.$$

Table 2
Example 6.2, model (27) - Empirical order of convergence.

n	$e_n(u)$	EOC_n
8	9.40e-03	
16	7.36e-04	3.68
32	6.61e-05	3.48
64	6.68e-06	3.31
128	1.87e-07	5.16
256	3.30e-09	5.82
512	2.56e-10	3.69
$\mathrm{EOC}_{\mathrm{mean}}$		4.19

Table 3
Example 6.3, model (28) - Empirical order of convergence.

n	$e_n(u)$	EOC_n
8	1.47e-02	
16	1.27e-04	6.85
32	9.12e-06	3.80
64	3.56e-06	1.36
128	3.32e-07	3.42
256	2.34e-09	7.15
512	3.85e-10	2.60
$\mathrm{EOC}_{\mathrm{mean}}$		4.20

Example 6.2.

$$\begin{aligned} u(x,t) &= x + t^2, \\ r = \frac{1}{\pi}, \quad \varphi(y-x) &= e^{-(y-x)}, \quad m(x) = \log(x^2+1), \\ u(\boldsymbol{x},0) = (x_0,\dots,x_n), \quad u(-a,t) &= -a + t^2, \quad u(a,t) = a + t^2. \end{aligned} \tag{27}$$

Example 6.3.

$$\begin{aligned} u(x,t) &= e^{x+\frac{t}{5}}, \\ r = \frac{1}{3}, \quad \varphi(y-x) &= \cos^2(y-x), \quad m(x) = -\frac{x^2}{2} + 4, \\ u(\boldsymbol{x},0) = (e^{x_0},\dots,e^{x_n}), \quad u(-a,t) &= e^{-a+\frac{t}{5}}, \quad u(a,t) = e^{a+\frac{t}{5}}. \end{aligned} \tag{28}$$

6.2. *Numerical simulations in the context of population theory*

After testing the reliability of the proposed numerical schemes, in the next examples we perform further simulations for cases in which the analytical solution $u(x,t)$ is not known, but investigating the results behaviour as function of the model parameters and functions. Namely, the reproduction rate r, the integral $\mathcal{K}(u,x,t)$, the mortality function $m(x)$ and the initial and Dirichlet boundary conditions $k(x)$ and $b_{\pm}(t)$ respectively. In this context, we assume that $u(x,t)$ and $\varphi(y-x)$ are non-negative functions. In particular, the former in this context represents population values.

Example 6.4.

$$\begin{aligned} r = \frac{1}{7}, \quad \varphi(y-x) &= 2 + \sin(y-x), \quad m(x) = \log(x+3), \\ u(\boldsymbol{x},0) = (0,\dots,0), \quad u(-a,t) &= u(a,t) = a^2 t. \end{aligned} \tag{29}$$

Let us consider Example 6.4. In this case the reproduction rate r is equal to $\frac{1}{7}$, while the mortality function $m(x)$ has a logarithmic behaviour with a minimum at the endpoint $x = -a$ and a maximum at $x = a$. Finally, the Dirichlet boundary conditions are the same, both linear in time. The numerical solution $\hat{u}(x,t)$ for this reference problem (29) is displayed in Fig. 1 (a).

We now investigate how the solution is influenced by a change in the initial conditions and the Dirichlet boundary conditions. In Fig. 1 (b) we note that for $u(\boldsymbol{x},0) = (3,\dots,3)$ and $b_{\pm}(t) = 3e^{\sqrt{t}}$, there is an exponential increase of the population at the endpoints.

Moreover, in the first half of the space interval, the population is more prolific than the one of the reference problem, while in the other half, we witness higher mortality, in line with the chosen mortality function. Fig. 1 (c) displays a reduction of the population, due to a lower value of its reproduction rate r, which is in this case equal to $\frac{1}{25}$. The opposite situation is highlighted by Fig. 1 (d), where $r = \frac{1}{5}$ and the population has a peak of growth in the interval $[-2, 0]$, while in the other half of the interval has a weaker increase due to the mortality $m(x) = \log(x+3)$. Hence, we proceed to consider different mortality functions in the last two plots of Fig. 1. In (e) the chosen function is $m(x) = -\frac{x^2}{2} + 4$, which has a peak at $x = 0$. This behaviour leads to a general decrease in the population, in particular around that point. We note a different situation in Fig. 1 (f) where $m(x) = \frac{x^2}{2} + 1$. In this case, the mortality is higher at the endpoints and lower in the middle of the space interval. Hence, the increase of the population in the neighbourhood of the endpoints can only be ascribed to the boundary conditions $u(-a,t) = u(a,t) = a^2 t$.

Example 6.5.

$$r = \frac{1}{4}, \quad \varphi(y-x) = 1 + \sin(25(y-x)), \quad m(x) = \log^3(x+3), \tag{30}$$
$$u(\boldsymbol{x}, 0) = (1, \dots, 1), \quad u(-a,t) = u(a,t) = e^{\sqrt{t}}.$$

Fig. 2 depicts the results for Example 6.5. The reference problem (30) is displayed in frame (a). It describes a population with higher mortality at the centre of the space interval and an exponential increase at the endpoints of the interval. This time the reproduction rate is equal to $\frac{1}{4}$, the mortality function is $m(x) = \log^3(x+3)$ and the kernel $\varphi(y-x)$ is highly oscillating. Fig. 2 (b) considers the case in which the Dirichlet boundary conditions are again the same and both impose an exponential decrease in the population at the endpoints of the space interval. This assumption leads to the extinction of the population, although at the beginning of the time interval there is a slight increase due to the contribution of the oscillating kernel φ in $\mathcal{K}(u,x,t)$. We point out that the scale used for the z-axis of this plot is different from the other ones in Fig. 2 only to allow the reader to observe easily the behaviour of the population in this context. This remark applies also to the Figs. 3 (b) and 4 (b) of the next two examples. In Fig. 2 (c) and Fig. 2 (d) we consider an increase and a decrease in the reproduction rate respectively. In the first case the reproduction rate is $r = \frac{1}{3}$, leading the population to reduce its mortality in the interval $[0,2]$ and to have a significant increase in $[-2,0]$ with respect to the reference problem. The second case shows how the reproduction rate is so low that the mortality is higher essentially everywhere, with the clear exception of the neighbourhood of the points $x = -a$, a due to the imposed boundary conditions. Figs. 2 (e) and (f) show the reaction of the population $u(x,t)$ to two different mortality functions $m(x)$. In both cases we have a decrease of the population with respect to the reference problem, with a higher mortality in (e) caused by a peak of the function $m(x) = e^{-x^2+2}$ in $x = 0$, except for the endpoints where the mortality almost vanishes.

Example 6.6.

$$r = \frac{1}{10}, \quad \varphi(y-x) = e^{-(y-x)}, \quad m(x) = e^{-\frac{x}{2}}, \tag{31}$$
$$u(\boldsymbol{x}, 0) = (1, \dots, 1), \quad u(-a,t) = u(a,t) = \frac{t^2}{2} + 1.$$

We focus now on Example 6.6. This time the reproduction rate is $r = \frac{1}{10}$, the kernel $\varphi(y-x) = e^{-(y-x)}$ and the mortality $m(x) = e^{-\frac{x}{2}}$ have exponential decay, while the Dirichlet boundary conditions are $b_{\pm}(t) = \frac{t^2}{2} + 1$, in agreement with the initial conditions $u(\boldsymbol{x}, 0) = (1, \dots, 1)$. The growth of the population among the time interval $[0, 25]$ in this reference problem (31) is displayed by Fig. 3 (a). We observe a significant increase in the population in the interval $[1,2]$, while around the point $x = -1$ a slower growth is observed. This is not surprising, since the mortality is higher in the first half of the space interval, decreasing exponentially in space. The only factor that ensures a stronger growth at $x = -2$ is the boundary condition $b\_(t)$, essentially prevailing on the contribution of $m(x)$ there. Fig. 3 (b) considers the case in which the boundary condition is oscillating, i.e. $b_{\pm}(t) = \sin^2\left(\frac{t}{5}\right)$. In this context, we note a behaviour of the population growth similar to the one of the reference problem in the space interval, but reiterated in time due to the nature of the functions $b_{\pm}(t)$. The peak we observed in (a) is even higher in Fig. 3 (c) when the reproduction rate r is increased to $\frac{1}{8}$. We have a similar situation, but with a slower growth rate in Fig. 3 (d), where $r = \frac{1}{15}$. This occurrence can easily be explained by the nature of the mortality function $m(x)$. Indeed, the consideration of a different one, as in the case of Fig. 3 (e), where $m(x) = e^{-\frac{x^2}{2}} + 2$, leads to a drastic change where the peaks of growth are guaranteed only by the boundary conditions $b_{\pm}(t)$, while the mortality gives a significant slowdown to the population growth at the centre of the space interval. Finally, Fig. 3 (f) displays a behaviour analogous to the one we just described, with an even stronger decrease in the population near the spatial endpoints.

Example 6.7.

$$r = \frac{1}{5}, \quad \varphi(y-x) = \cos^2(y-x), \quad m(x) = e^{-\frac{x}{3}}, \tag{32}$$
$$u(\boldsymbol{x}, 0) = (3, \dots, 3), \quad u(-a,t) = e^{-\frac{t}{a^2}} + 2, \quad u(a,t) = e^{\frac{t}{a^2}} + 2.$$

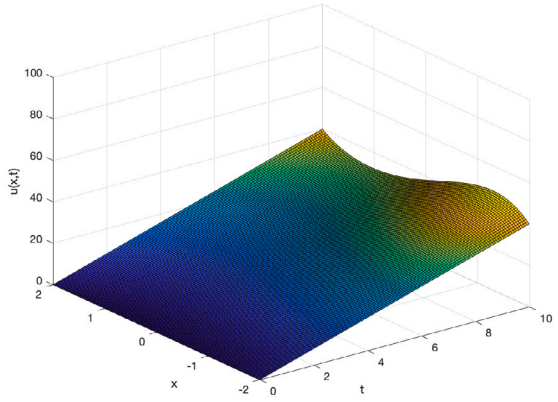

(a) Reference problem (29): $r = \frac{1}{7}$, $\varphi(y-x) = 2 + \sin(y-x)$, $m(x) = \log(x+3)$, $u(\boldsymbol{x}, 0) = (0, \ldots, 0)$, $b_{\pm}(t) = a^2 t$.

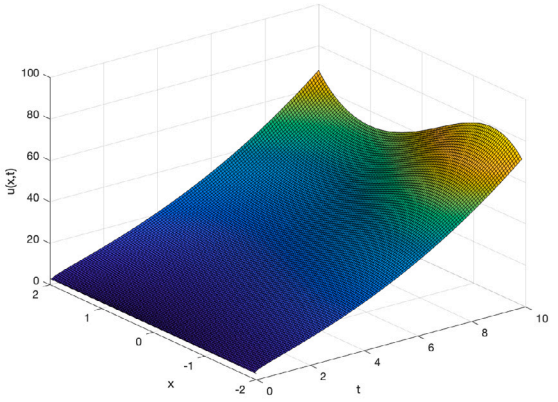

(b) $u(\boldsymbol{x}, 0) = (3, \ldots, 3)$, $b_{\pm}(t) = 3e^{\sqrt{t}}$

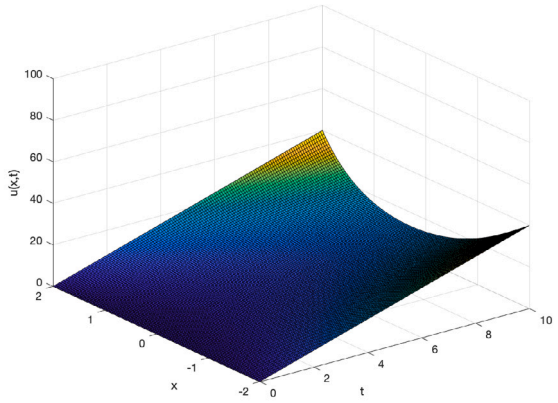

(c) $r = \frac{1}{25}$

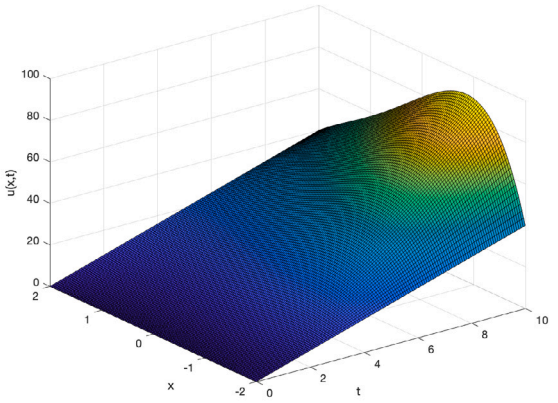

(d) $r = \frac{1}{5}$

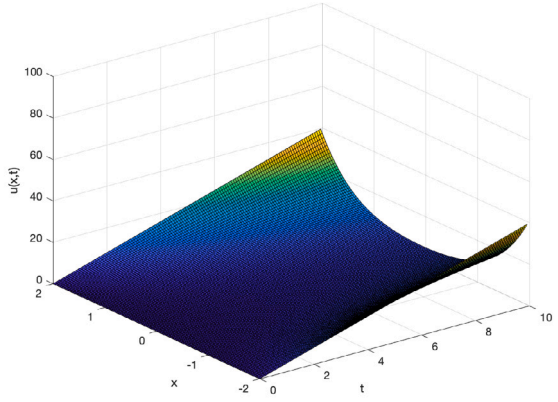

(e) $m(x) = -\frac{x^2}{2} + 4$

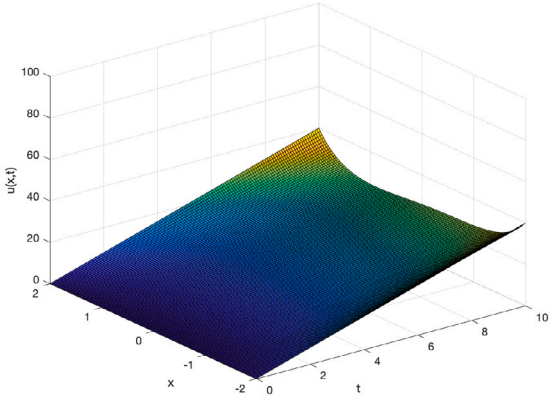

(f) $m(x) = \frac{x^2}{2} + 1$

Fig. 1. Example 6.4.

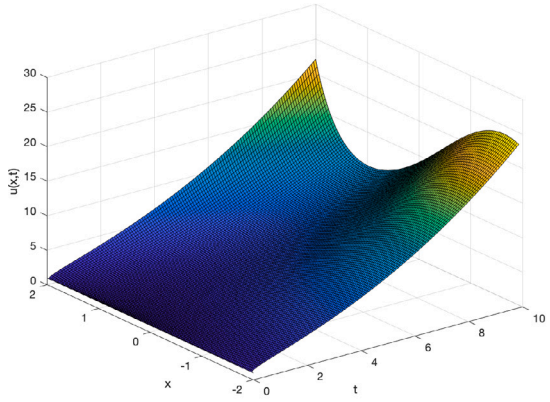

(a) Reference problem (30): $r = \frac{1}{4}$, $\varphi(y-x) = 1 + \sin(25(y-x))$, $m(x) = \log^3(x+3)$, $u(\boldsymbol{x},0) = (1,\ldots,1)$, $b_{\pm}(t) = e^{\sqrt{t}}$.

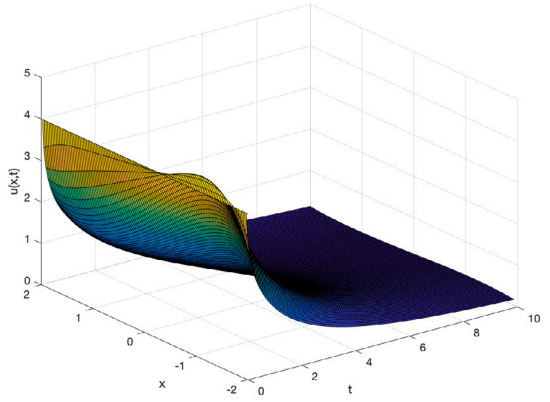

(b) $u(\boldsymbol{x},0) = (a^2,\ldots,a^2)$, $b_{\pm}(t) = a^2 e^{-\sqrt{t}}$

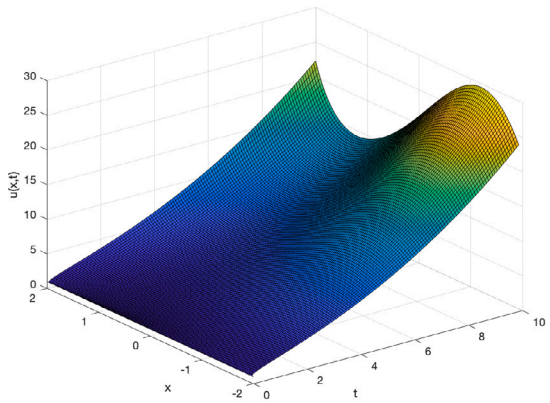

(c) $r = \frac{1}{3}$

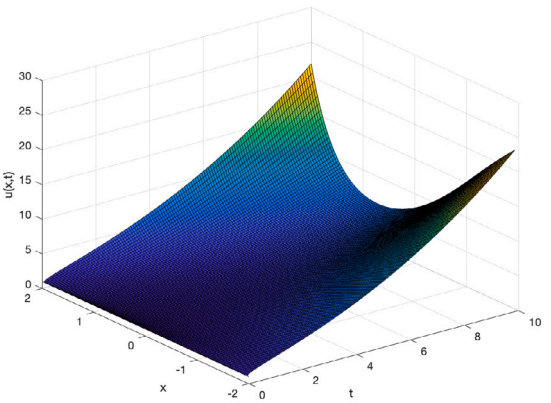

(d) $r = \frac{1}{8}$

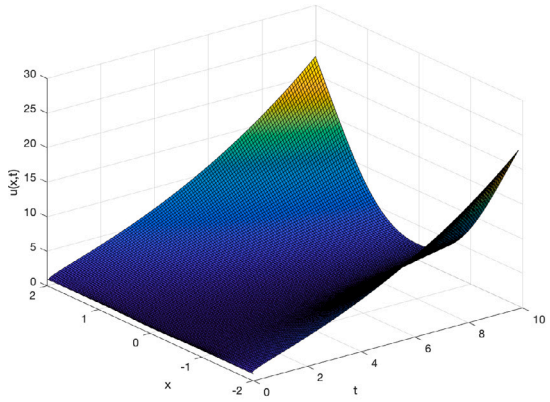

(e) $m(x) = e^{-x^2+2}$

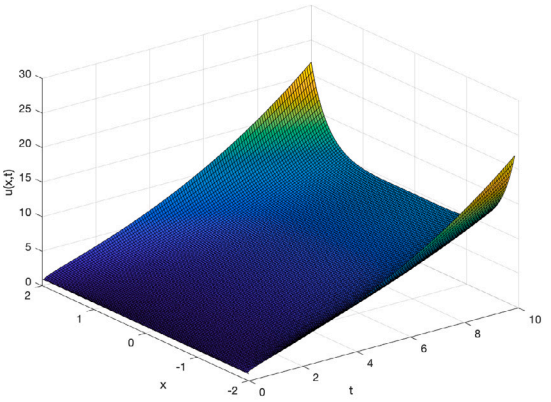

(f) $m(x) = e^{\frac{x^2}{2}}$

Fig. 2. Example 6.5.

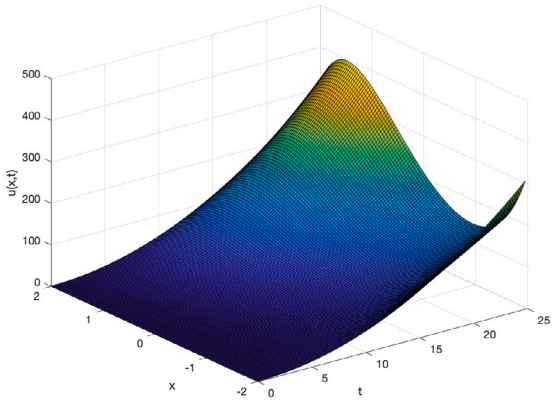

(a) Reference problem (31): $r = \frac{1}{10}$, $\varphi(y-x) = e^{-(y-x)}$, $m(x) = e^{-\frac{x}{2}}$, $u(\boldsymbol{x},0) = (1,\ldots,1)$, $b_{\pm}(t) = \frac{t^2}{2} + 1$.

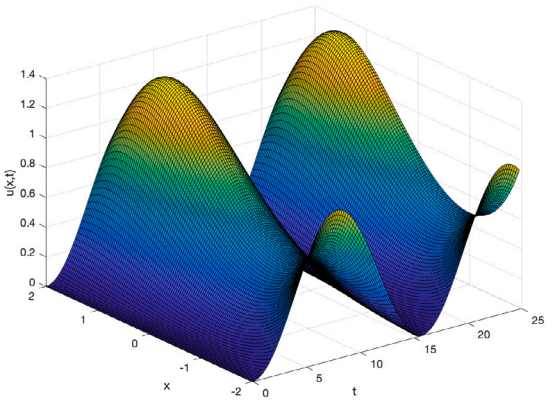

(b) $u(\boldsymbol{x},0) = (0,\ldots,0)$, $b_{\pm}(t) = \sin^2\left(\frac{t}{5}\right)$

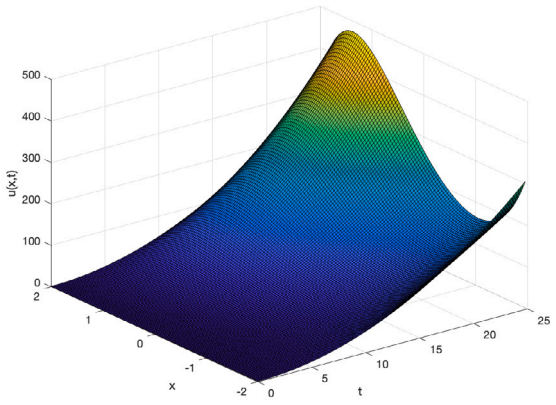

(c) $r = \frac{1}{8}$

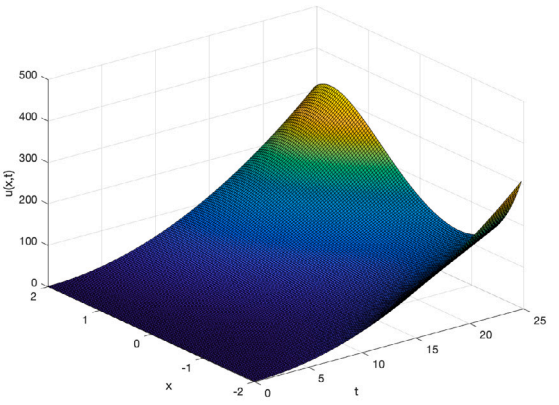

(d) $r = \frac{1}{15}$

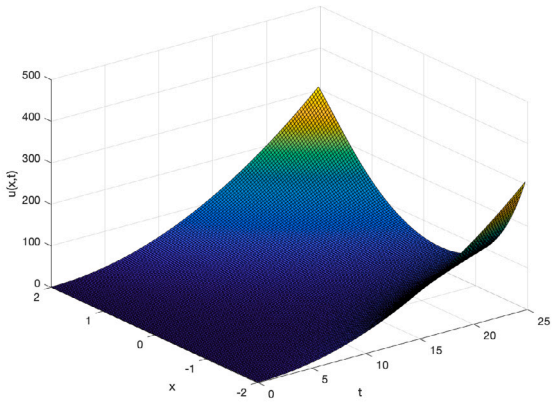

(e) $m(x) = e^{-\frac{x^2}{2}} + 2$

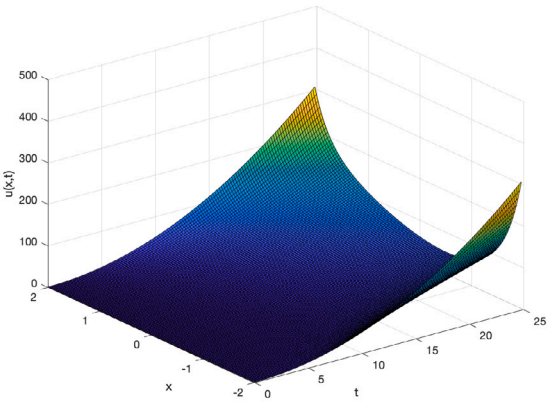

(f) $m(x) = e^{\frac{x^2}{2}} + 1$

Fig. 3. Example 6.6.

Table 4
Example 6.4, model (29) - Empirical order of convergence.

n	$e_n(u)$	EOC_n
8	4.53e-03	
16	3.78e-04	3.58
32	2.35e-05	4.01
64	1.15e-06	4.35
128	3.59e-07	4.09
256	2.08e-08	4.11
$\mathrm{EOC}_{\mathrm{mean}}$		4.03

We conclude our numerical simulations for the model with Example 6.7, whose plots are shown in Fig. 4. In this last example, we are dealing with the case of different Dirichlet boundary conditions, namely $b_-(t) = e^{-\frac{t}{a^2}} + 2$ and $b_+(t) = e^{\frac{t}{a^2}} + 2$ respectively. Moreover, we consider the space interval $[-3, 3]$ and the time interval $[0, 15]$ and set our reference problem (32) with the reproduction rate $r = \frac{1}{5}$, the kernel function $\varphi(y-x) = \cos^2(y-x)$ and the mortality $m(x) = e^{-\frac{x}{3}}$. In Fig. 4 (a) we note a peak at the endpoint $x = 3$ due to the boundary condition $b_+(t)$ and to the mortality almost vanishing at that boundary. The situation is totally reversed in the first half of the space interval, causing a reduction of the population due to the higher mortality. Also in this example, we replace the reference boundary conditions with two identical oscillating functions, namely $b_\pm(t) = 3\cos^2\left(\frac{t}{2}\right)$. As in the previous example, Fig. 4 (b) shows a behaviour that is similar to the one shown in the reference problem, with the exception that in this case this pattern is iterated following the behaviour of the new boundary conditions. Fig. 4 (c) displays the case in which the reproduction rate $r = \frac{1}{\pi}$ is higher than the one in (a), leading to a general reduction of the mortality in the whole space interval. The situation is reversed in Fig. 4 (d) where the reproduction rate decreases to $\frac{1}{15}$, so that the mortality in the first half of the interval prevails with respect to the situation depicted in (a). The same considerations hold for Fig. 4 (e) where the mortality function is $m(x) = -\frac{x^2}{3} + 3$ and hence the population is preserved from disappearing at the endpoints $x = \pm 3$. Finally, Fig. 4 (f) assumes that the mortality is given by $m(x) = \frac{x^2}{3}$. This implies that the population does not vanish near the centre of the space interval, leading to its significant growth as time flows. We have the opposite situation near the endpoints, where at $x = 3$ the population is reduced due to the Dirichlet boundary condition $b_+(t)$.

Note that in all examples of this subsection the analytic solution is not known. However, we can try to give an estimate of the order of convergence using the following scheme.

To evaluate MEOC in this context we compute the following relative error

$$\epsilon_n(u) = \sup_{t\in[0,T]} \max_{x\in[-a,a]} \frac{|\hat{u}_{2n}(x,t) - \hat{u}_n(x,t)|}{|\hat{u}_{2n}(x,t)|},$$

$$\mathrm{EOC}_n = \frac{\log\left(\frac{\epsilon_{n/2}(u)}{\epsilon_n(u)}\right)}{\log 2}, \quad \mathrm{EOC}_{\mathrm{mean}} = \frac{1}{P-2}\sum_{k=3}^{P} \mathrm{EOC}_{2^k}.$$

Applying these formulae, for instance, to Example 6.4, we obtain the numerical results shown in Table 4. Also in this case the theoretical expectations are confirmed, and the Mean Empirical Order of Convergence is once again around 4.

7. Conclusions

In this paper, we provided a method for the integration of a nonlinear reaction-diffusion equation in a biological context arising in population theory. We investigated its convergence, obtaining as main result that it is of the fourth order. The theoretical findings were confirmed by several numerical examples. Motivated by the good (preliminary) results achieved in this one-dimensional case, our future goal is to extend this method to the case of more realistic two- and three-dimensional models, that respectively describe the long distance intraspecific competition for food supplies. The former case concerns biological populations that live on the ground, the latter instead considers the aquatic or aereal environments, i.e. shoals of fish and flocks of birds.

Acknowledgements

EV has been partially supported by the project “Metodi di approssimazione e modelli per le scienze della vita” (Approximation methods and models for the life sciences) of the Department of Mathematics “Giuseppe Peano” of the University of Turin. DM has been partially supported by GNCS-INdAM 2023 project “Approssimazione ed integrazione multivariata con applicazioni ad equazioni integrali”. DO has been partially supported by PRIN 2022 PNRR project no. P20229RMLB financed by the European Union - NextGeneration EU and by the Italian Ministry of University and Research (MUR). This research has been accomplished within RITA (Research ITalian network on Approximation) and the UMI Group TAA (Approximation Theory and Applications).

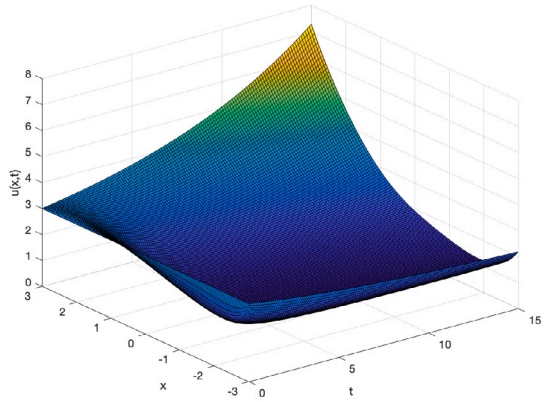

(a) Reference problem (32): $r = \frac{1}{5}$, $\varphi(y-x) = \cos^2(y-x)$, $m(x) = e^{\frac{x}{2}}$, $u(\boldsymbol{x},0) = (1,\ldots,1)$, $b_{\pm}(t) = e^{\pm\frac{t}{a^2}} + 2$.

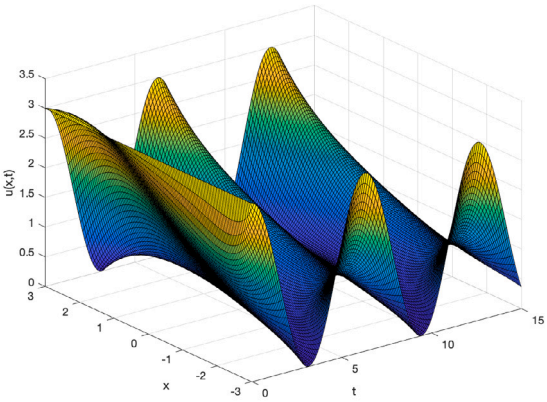

(b) $u(\boldsymbol{x},0) = (3,\ldots,3)$, $b_{\pm}(t) = 3\cos^2\left(\frac{t}{2}\right)$

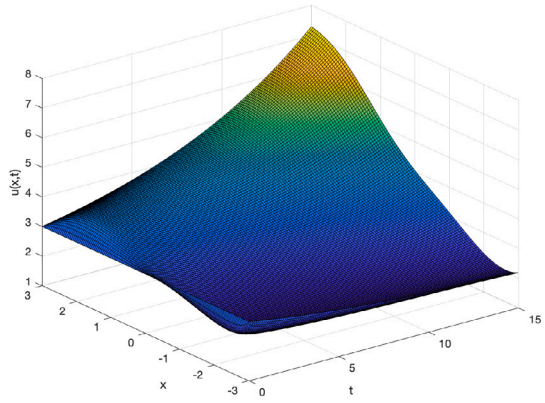

(c) $r = \frac{1}{\pi}$

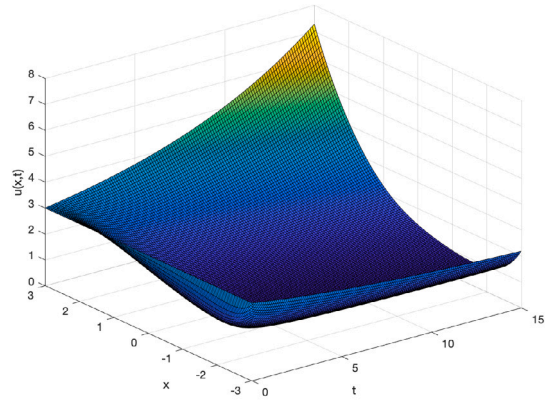

(d) $r = \frac{1}{7}$

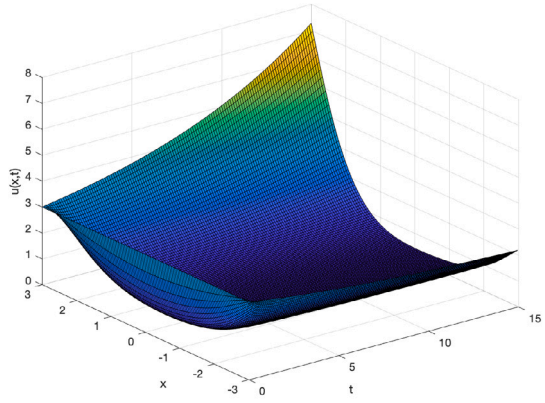

(e) $m(x) = -\frac{x^2}{3} + 3$

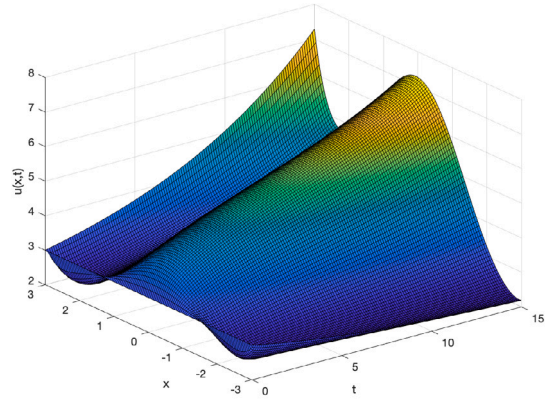

(f) $m(x) = \frac{x^2}{3}$

Fig. 4. Example 6.7.

References

[1] N. Apreutesei, A. Ducrot, V. Volpert, Competition of species with intra-specific competition, Math. Model. Nat. Phenom. 3 (4) (2008) 1–27.
[2] K.E. Atkinson, An Introduction to Numerical Analysis, Wiley, NY, 1978.
[3] K.E. Atkinson, Elementary Numerical Analysis, Wiley, NY, 1993.
[4] M. Banerjee, S.V. Petrovskii, V. Volpert, Nonlocal reaction-diffusion models of heterogeneous wealth distribution, Mathematics 9 (4) (2021) 1–18.
[5] A. Baskaran, Z. Hu, J.S. Lowengrub, C. Wang, S.M. Wise, P. Zhou, Energy stable and efficient finite-difference nonlinear multigrid schemes for the modified phase field crystal, J. Comput. Phys. 250 (2013) 270–292.
[6] P.W. Bates, A.J.J. Chmaj, An integrodifferential model for phase transitions: stationary solutions in higher space dimensions, J. Stat. Phys. 95 (1999) 1119–1139.
[7] P.W. Bates, J. Han, Neumann boundary problem for the nonlocal Cahn-Hilliard equation, J. Differ. Equ. 212 (2) (2005) 235–277.
[8] P.W. Bates, J. Han, The Dirichlet boundary problem for the nonlocal Cahn-Hilliard equation, J. Math. Anal. Appl. 311 (1) (2005) 289–312.
[9] P.W. Bates, On some nonlocal evolution equations arising in materials science. Nonlinear dynamics and evolution equations, Fields Inst. Commun. 48 (2006) 13–52.
[10] P.W. Bates, J. Han, G. Zhao, On a nonlocal phase-field system, Nonlinear Anal., Theory Methods Appl. 64 (10) (2006) 2251–2278.
[11] P.W. Bates, S. Brown, J. Han, Numerical analysis for a nonlocal Allen-Cahn equation, Int. J. Numer. Anal. Model. 6 (1) (2009) 33–49.
[12] E. Bellavere, E. Venturino, Crossing the desert: a model for alien species invasion containment or to lessen habitat disruption effects, J. Biol. Syst. 31 (2) (2023) 557–589.
[13] N. Bessonov, G. Bocharov, A. Mozokhina, V. Volpert, Viral infection spreading in cell culture with intracellular regulation, Mathematics 11 (6) (2023).
[14] M. Campiti, Convergence of iterated Boolean-type sums and their iterates, Numer. Funct. Anal. Optim. 39 (10) (2018) 1054–1063.
[15] X. Chen, Existence, uniqueness, and asymptotic stability of traveling waves in non- local evolution equations, Adv. Differ. Equ. 2 (1) (1997) 125–160.
[16] A.J.J. Chmaj, X. Ren, Multiple solutions of the nonlocal bistable equation, Physica D 147 (2000) 135–154.
[17] A.J.J. Chmaj, X. Ren, Pattern formation in the nonlocal bistable equation, Methods Appl. Anal. 8 (2001) 369–386.
[18] S. Cooper, S. Waldron, The eigenstructure of the Bernstein operator, J. Approx. Theory 105 (2000) 133–165.
[19] C. Cortazar, M. Elgueta, J.D. Rossi, Nonlocal diffusion problems that approximate the heat equation with Dirichlet boundary conditions, Isr. J. Math. 170 (2009) 53–60.
[20] C.M. Elliott, S. Zheng, On the Cahn-Hilliard equation, Arch. Ration. Mech. Anal. 96 (1986) 339–357.
[21] G. Farin, Curves and Surfaces for Computer-Aided Geometric Design, third edition, Academic Press, 1993.
[22] L. Fermo, D. Mezzanotte, D. Occorsio, A product integration rule on equispaced nodes for highly oscillating integrals, Appl. Math. Lett. 136 (2023) 108463.
[23] R.A. Fisher, The wave of advance of advantageous genes, Ann. Hum. Genet. 7 (4) (1937) 355–369.
[24] B. Fornberg, Generation of finite difference formulas on arbitrarily spaced grids, Math. Comput. 51 (184) (1988) 699–706.
[25] S. Genieys, V. Volpert, P. Auger, Pattern and waves for a model in population dynamics with nonlocal consumption of resources, Math. Model. Nat. Phenom. 1 (1) (2006) 63–80.
[26] S.A. Gourley, Travelling front solutions of a nonlocal Fisher equation, J. Math. Biol. 41 (3) (2000) 272–284.
[27] A.N. Kolmogorov, I.G. Petrovsky, N.S. Piskunov, Étude de l'équation de la diffusion avec croissance de la quantité de matière et son application à un problème biologique, Bull. Moskov. Gos. Univ. Mat. Mekh. 1 (6) (1937).
[28] A.J. Lotka, Elements of Mathematical Biology, Dover, New York, 1956.
[29] H. Malchow, S. Petrovskii, E. Venturino, Spatiotemporal Patterns in Ecology and Epidemiology, CRC, 2008.
[30] T.R. Malthus, An Essay on the Principle of Population, J. Johnson in St. Paul's Churchyard, London, 1798.
[31] D. Mezzanotte, D. Occorsio, M.G. Russo, E. Venturino, A discretization method for nonlocal diffusion type equations, Ann. Univ. Ferrara 68 (2) (2022) 505–520.
[32] A. Moussaoui, V. Volpert, Speed of wave propagation for a nonlocal reaction-diffusion equation, Appl. Anal. 99 (13) (2020) 2307–2321.
[33] J.D. Murray, Mathematical Biology, Springer, Berlin, 1989.
[34] D. Occorsio, Some new properties of generalized Bernstein polynomials, Stud. Univ. Babeş–Bolyai, Math. 56 (2011) 147–160.
[35] D. Occorsio, M.G. Russo, Nyström methods for Fredholm integral equations using equispaced points, Filomat 28 (1) (2014) 49–63.
[36] D. Occorsio, M.G. Russo, W. Themistoclakis, Some numerical applications of generalized Bernstein operators, Constr. Math. Anal. 4 (2) (2021) 186–214.
[37] M.J. Simpson, N. Rahman, S.W. McCue, A.K.Y. Tam, Survival, extinction, and interface stability in a two-phase moving boundary model of biological invasion, Phys. D, Nonlinear Phenom. 456 (2023) 133912.
[38] S. Trofimchuk, V. Volpert, Traveling waves in delayed reaction-diffusion equations in biology, Math. Biosci. Eng. 17 (6) (2020) 6487–6514.
[39] P.F. Verhulst, Recherches mathématiques sur la loi d'accroissement de la population, Mém. Acad. R. Brux. 18 (1845) 1–45.
[40] A.I. Volpert, V. Volpert, V.A. Volpert, Traveling Wave Solutions of Parabolic Systems, Translations of Mathematical Monographs, vol. 140, Amer. Math. Society, Providence, 1994.
[41] V. Volterra, U. D'Ancona, La concorrenza vitale tra le specie dell'ambiente marino (vital competition among species in the aquaticenvironment), in: VIIe Congr. Int. Acquicult et de Pêche, Paris, 1931, pp. 1–14.
[42] V. Vougalter, V. Volpert, Solvability of some systems of integro-differential equations in population dynamics depending on the natality and mortality rates, Arnold Math. J. (2023).